ISSN 1674-1056
http://cpb.iphy.ac.cn
http://iopscience.iop.org/cpb
中国物理 B
Chinese Physics
中国物理 Chinese Physics B

Magnetic field analysis in a diamond anvil cell for Meissner effect measurement by using the diamond NV$^-$ center

Lin Zhao(赵琳), Donghui Yue(岳冬辉), Cailong Liu(刘才龙), Min Wang(王敏), Yonghao Han(韩永昊), Chunxiao Gao(高春晓)

Citation: Chin. Phys. B . 2019, 28(3): 030702. **doi:** 10.1088/1674-1056/28/3/030702
Journal homepage: http://cpb.iphy.ac.cn; http://iopscience.iop.org/cpb

What follows is a list of articles you may be interested in

Damage and recovery of fiber Bragg grating under radiation environment

Shi-Zhe Wen(温世喆), Wei-Chen Xiong(熊伟晨), Li-Ping Huang(黄力平), Zhen-Rui Wang(王镇锐), Xing-Bin Zhang(张兴斌), Zhen-Hui He(何振辉)

Chin. Phys. B . 2018, 27(9): 090701. **doi:** 10.1088/1674-1056/27/9/090701

Highly-sensitive NO, NO_2, and NH_3 measurements with an open-multipass cell based on mid-infrared wavelength modulation spectroscopy

Xiang Chen(陈祥), Chen-Guang Yang(杨晨光), Mai Hu(胡迈), Jian-Kang Shen(沈建康), Er-Chao Niu(牛二超), Zhen-Yu Xu(许振宇), Xue-Li Fan(范雪丽), Min Wei(魏敏), Lu Yao(姚路), Ya-Bai He(何亚柏), Jian-Guo Liu(刘建国), Rui-Feng Kan(阚瑞峰)

Chin. Phys. B . 2018, 27(4): 040701. **doi:** 10.1088/1674-1056/27/4/040701

High-pressure synchrotron x-ray diffraction and Raman spectroscopic study of plumbogummite

Duan Kang(康端), Xiang Wu(巫翔), Guan Yuan(袁冠), Sheng-Xuan Huang(黄圣轩), Jing-Jing Niu(牛菁菁), Jing Gao(高静), Shan Qin(秦善)

Chin. Phys. B . 2018, 27(1): 017402. **doi:** 10.1088/1674-1056/27/1/017402

High-pressure Raman study of solid hydrogen up to 300 GPa

Xiaoli Huang(黄晓丽), Fangfei Li(李芳菲), Yanping Huang(黄艳萍), Gang Wu(吴刚), Xin Li(李鑫), Qiang Zhou(周强), Bingbing Liu(刘冰冰), Tian Cui(崔田)

Chin. Phys. B . 2016, 25(3): 037401. **doi:** 10.1088/1674-1056/25/3/037401

Magnetic transition of ferromagnetic material at high pressure using a novel system

Hu Tian-Li, Wang Xin, Han Bing, Li Yan, Huang Feng-Xian, Zhou Qiang, Zhang Tao

Chin. Phys. B . 2013, 22(12): 120701. **doi:** 10.1088/1674-1056/22/12/120701

Magnetic field analysis in a diamond anvil cell for Meissner effect measurement by using the diamond NV$^-$ center*

Lin Zhao(赵琳), Donghui Yue(岳冬辉), Cailong Liu(刘才龙),
Min Wang(王敏), Yonghao Han(韩永昊)†, and Chunxiao Gao(高春晓)

State Key Laboratory of Superhard Materials, Jilin University, Changchun 130012, *China*

(Received 28 November 2018; revised manuscript received 9 January 2019; published online 26 February 2019)

Diamond negatively charged nitrogen-vacancy (NV$^-$) centers provide an opportunity for the measurement of the Meissner effect on extremely small samples in a diamond anvil cell (DAC) due to their high sensitivity in detecting the tiny change of magnetic field. We report on the variation of magnetic field distribution in a DAC as a sample transforms from normal to superconducting state by using finite element analysis. The results show that the magnetic flux density has the largest change on the sidewall of the sample, where NV$^-$ centers can detect the strongest signal variation of the magnetic field. In addition, we study the effect of magnetic coil placement on the magnetic field variation. It is found that the optimal position for the coil to generate the greatest change in magnetic field strength is at the place as close to the sample as possible.

Keywords: negatively charged nitrogen-vacancy (NV$^-$) centers, diamond anvil cell, superconductivity, magnetic field detection

PACS: 07.07.Df, 07.55.Ge, 74.20.–Z, 02.70.Dh **DOI:** 10.1088/1674-1056/28/3/030702

1. Introduction

Pressure-induced superconductivity in materials has always attracted much interest from scientists.[1,2] Recently, a new record of superconducting transition temperature (T_c) of 203 K at 150 GPa was achieved in H_2S,[3–5] and enthusiasm for pursuing high T_c values under high pressures will last without any reduction till the final goal of room-temperature superconductivity is realized in compressed hydrogen.[6] To reach the goal, zero resistance and Meissner effect measurements must be fulfilled in a diamond anvil cell (DAC).[7,8] However, both of them have technical limitations on very tiny samples under pressure,[9] e.g., for zero resistance measurement, direct contact between the electrodes and samples is required,[10,11] however the electrodes are likely to react with the sample under ultrahigh pressures, forming unexpected compounds and making it difficult to effectively determine the superconductivity; Meissner effect measurement with magnetic coils requires sufficiently strong signals of diamagnetism, which are also very difficult to obtain for a sample of which diameter is only a few microns under several megabars.[12] Therefore, it is essential to develop a technique in a DAC to solve the above problems and make it possible to effectively determine the pressure-induced superconductivity in a very tiny sample.

Recently, the electron spin resonance (ESR) technique based on the negatively charged nitrogen-vacancy (NV$^-$) center is expected to play a key role in detecting the diamagnetism signals of superconducting samples in a DAC.[12–14] The NV$^-$ center is a point defect comprising a substitutional nitrogen atom and an adjacent crystallographic vacancy and has degenerate triplet electronic ground state $^3A_2$ ($m_s = 0$ and $m_s = \pm 1$).[15,16] When electrons are de-excited from excited state ^3E to the ground state, photons with energy 1.945 eV and fluorescence wavelength 637 nm are radiated.[14] If a microwave of frequency 2.87 GHz is introduced near the NV$^-$ center, magnetic dipole oscillations will be formed between $|m_s = 0\rangle$ and $|m_s = \pm 1\rangle$ sub-levels of the ground state, resulting in that part of the energy being released in the form of a non-radiative transition as electrons are de-excited from the excited state, namely, ESR occurs.[16–18] Correspondingly, the fluorescence intensity at the microwave frequency of 2.87 GHz is obviously lower than that at other frequencies and an ESR absorption peak can be observed if the fluorescence intensity versus microwave frequency is continuously scanned.[19] When an external magnetic field is applied, the degeneracy of $|m_s = \pm 1\rangle$ sublevels will be removed, causing the original resonance absorption peak to split into two, as shown in Fig. 1(b).[14–18] The relationship between the external magnetic field and the frequencies of the splitting peaks can be expressed as

$$(g\mu B)^2 = (1/3)(\omega_1^2 + \omega_2^2 - \omega_1\omega_2 - D^2) - E^2, \qquad (1)$$

where g is the Land/'e g-factor of the electron, μ is the Bohr magneton, B is the external magnetic field strength, ω_1 and ω_2 are the angular frequencies of the splitting electron spin resonance peaks, $D = 2.87$ GHz, and E is the splitting parameter.[17] It can be seen from Eq. (1) that the splitting

*Project supported by the National Key R&D Program of China (Grant No. 2018YFA0305900) and the National Natural Science Foundation of China (Grant Nos. 11774126, 11674404, and 51772125).

†Corresponding author. E-mail: hanyh@jlu.edu.cn

© 2019 Chinese Physical Society and IOP Publishing Ltd

width of the absorption peaks, $(\omega_2 - \omega_1)$, is singularly determined by the external magnetic field strength.[20] The sudden change of the magnetic field therefore can be reflected by the splitting width of the absorption peaks,[21] which can be used to detect the onset of diamagnetism (the Meissner effect) in superconductors.

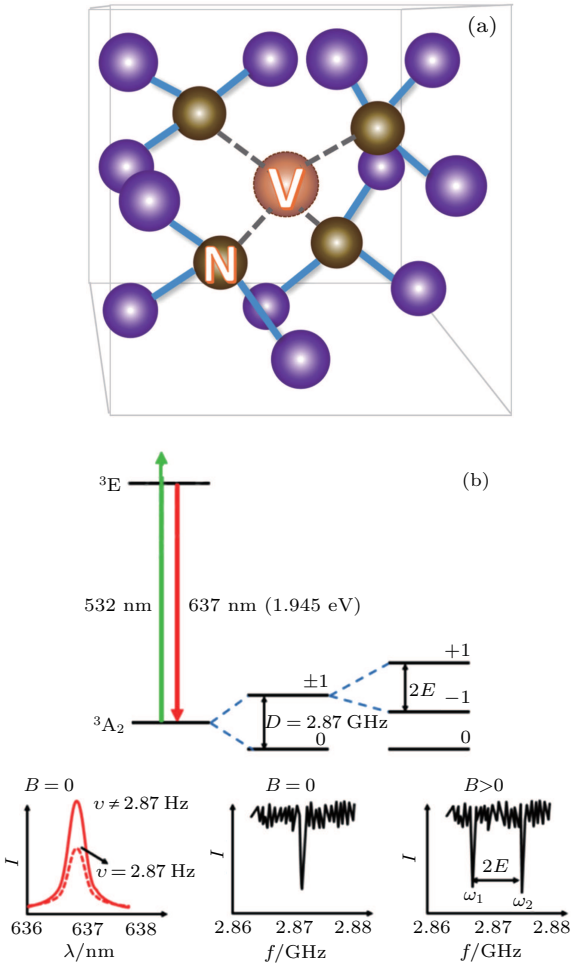


Fig. 1. (a) Structure diagram of the NV$^-$ center.[14,15] (b) Electron spin resonance schematic diagram. The NV ground-state spin sublevels are separated by $D = 2.87$ GHz, and $|m_s = \pm 1\rangle$ sublevels are degenerate, resulting in a single spin resonance frequency. In an external magnetic field, the degeneracy of $|m_s = \pm 1\rangle$ sublevels will be removed, resulting in two spin resonance frequencies.[14–18]

In real measurements, an exciting coil is needed to generate the external magnetic field. When a superconducting state appears, the Meissner effect makes the external field near the NV$^-$ center change. In order to maximize the sensitivity with which the NV- center detects the magnetic field variation, it is necessary to study the arrangements of the NV$^-$ center and the exciting coil on the DAC and the magnetic field distribution.

In this paper, the magnetic field distribution in a DAC before and after sample superconductivity was simulated. Samples with different permeability and exciting coils at different positions were considered. And then, the optimal arrangements of the NV$^-$ center and a reasonable configuration of the exciting coil were obtained at the end of the paper.

2. Theoretical models

Finite element analysis (FEA) is used to simulate the magnetic field distribution in a DAC as shown in Fig. 2. In real cases, the magnetic field for Meissner effect measurements can be provided directly by superconducting magnets in commercial cryogenic instruments or generated easily by hand-made coils. Considering that the generation and holding of high magnetic fields with superconducting magnets are high-cost and not all research groups can do the experiments at any time and any place, we adopt the second way, a hand-made coil to generate the magnetic field in the simulation. All the physical and geometrical properties of entities in FEA are input according to the real conditions in experiments.[22] The facet of the diamond anvil is 40 μm in diameter and the magnetic permeability of diamond is approximately 1 H/m. A rhenium gasket is used in simulation, whose size is 6 mm in diameter and 0.25 mm in thickness, and the magnetic permeability is 1 H/m. The gasket is dented to 3 μm in thickness and then a sample chamber with diameter 20 μm is drilled in the dent center. Three samples respectively with magnetic permeability of 1 H/cm, 100 H/cm, and 1000 H/cm are assumed to represent different materials. Herein, the magnetic permeability of 0 H/cm represents the sample in a superconducting state. The entities built in FEA are meshed with element PLANE 53. In order to generate a static magnetic field within the DAC, an exciting coil is placed around the diamond anvil and a magnetic vector potential $\boldsymbol{A} = 50$ mT·cm is applied. According to the magnetic vector potential method (MVP): $\boldsymbol{B} = \mathrm{Curl}(\boldsymbol{A})$, the magnetic flux intensity $\boldsymbol{B}$ can be calculated. The magnetic vector potential method has the advantage that there is no need to couple the current and voltage and the magnetic field excitation can be simulated in the simplest way.

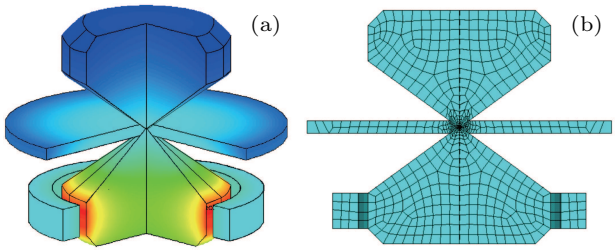


Fig. 2. Finite element analysis for magnetic field distribution in a DAC. (a) The entities built in the DAC and (b) the entities meshed by element PLANE 53 in two-dimensional simulation.

3. Analysis and discussion

The magnetic flux distribution in the DAC is shown in Fig. 3. The exciting coil is placed at the widest position close to the lateral edge of the diamond anvil. Figures 3(a)–3(c) are the simulation results for the samples with permeability 1000 H/cm, 100 H/cm, and 1 H/cm, respectively. Figure 3(d) is the simulation result for the sample having been converted into the superconductivity state. As the permeability of the

samples varies from 1000 H/cm to 0 H/cm, the holistic magnetic flux density distributions in the DAC are basically the same and the obvious difference only exists in the samples. As shown in Figs. 3(a) and 3(b), for magnetic samples with a permeability of 1000 H/cm and 100 H/cm, large magnetic field gradients can be observed inside the samples, and the maximum magnetic flux densities are 43.19 mT and 42.48 mT at the center of the sample sidewall, respectively. In Fig. 3(c), the magnetic field distribution within the non-magnetic sample (1 H/cm) is uniform, and the maximum magnetic flux density is 19.80 mT on the edge of the sample sidewall and near the exciting coil. While for the superconducting sample, as shown in Fig. 3(d), the internal magnetic flux density of the sample is 0 mT due to the Meissner effect. Previous results by Brandt can also be used to confirm the accuracy of our simulation results.[23] Therefore, it can be preliminarily concluded that, after the superconducting transition, the largest variation of magnetic flux density occurs at the center of the sample sidewall for magnetic samples and at the edge of the sample sidewall near the exciting coil for non-magnetic samples. Accordingly, the NV$^-$ center should be placed as close as possible to these positions.

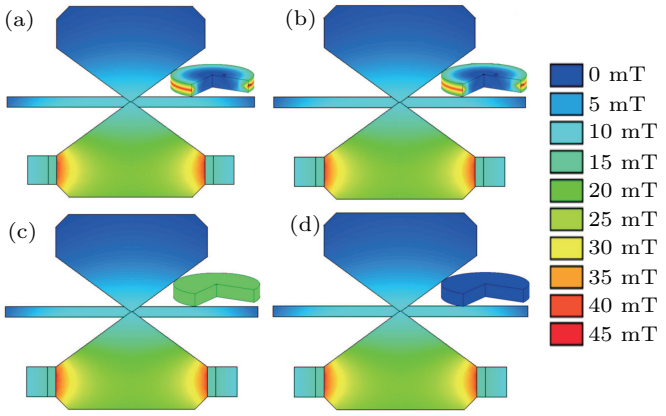


Fig. 3. Magnetic flux intensity distribution in the DAC, especially in the sample area. Panels (a)–(d) correspond to samples with different permeabilities of 1000 H/cm, 100 H/cm, 1 H/cm, and 0 H/cm, respectively.

In Eq. (1), it has been suggested that the sensitivity of the NV$^-$ center to the superconductivity depends on the variation of magnetic flux density as the sample transforms to a superconducting state. The arrangement of the exciting coil is another crucial factor for determining the magnetic flux density distribution in a DAC. A reasonable arrangement can maximize the magnetic flux density inside the sample, and correspondingly obtain the maximum variation of the magnetic flux density when the superconducting state appears.

Figure 4 shows the magnetic flux density distributions when the exciting coil is placed at different positions in the DAC. As an example, the magnetic permeability of the sample herein is set to 1000 H/cm and the magnetic vector potential $\boldsymbol{A} = 50$ mT·cm is applied on the exciting coil. For the coil on the gasket and as close to the sample as possible, as shown in Fig. 4(a), the maximum magnetic flux density at the center of the sample sidewall is 209.5 mT. When the coil departs away from the sample either horizontally or vertically, it can be clearly seen that the magnetic flux density decreases as shown in Figs. 4(b)–4(d). The optimized arrangement of the exciting coil therefore is that illustrated in Fig. 4(a).

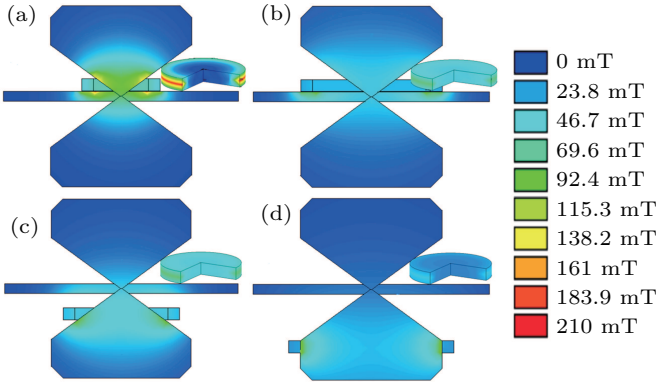


Fig. 4. Magnetic flux density distributions with different coil positions. The coil is (a) on the gasket and as close to the sample as possible, (b)–(d) moved away from the sample horizontally and vertically.

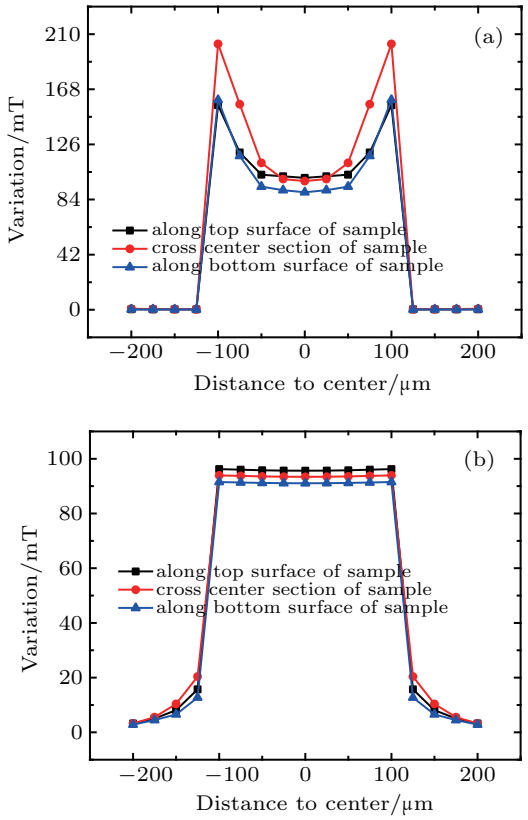


Fig. 5. The variations of magnetic flux intensity along the surfaces of different horizontal cross sections of the samples. The permeabilities of the samples are (a) 1000 H/cm and (b) 1 H/cm, respectively.

With the exciting coil arrangement in Fig. 4(a), the variation of the magnetic flux density is discussed successively for the magnetic (1000 H/cm) and non-magnetic (1 H/cm) samples when the superconducting transition occurs. Figure 5

shows the variations of magnetic flux intensity along the surfaces of different horizontal cross sections of the samples. It can be found that the most obvious variation of magnetic flux density occurs within the sample, while the magnetic flux density remains almost unchanged outside, which is consistent with the above discussion. For strong magnetic samples, the maximum of the magnetic flux density variation is on the center of the sample sidewall as shown in Fig. 5(a); for weak or non-magnetic samples, the difference among the variations of magnetic flux density in the sample is small. Therefore, either for magnetic samples or non-magnetic samples, placing the NV^- center on the edge of the sample is the optimal option.

4. Conclusion

The distribution of magnetic flux density in a DAC was analyzed for high-pressure Meissner effect measurement with the NV^- center. For both magnetic and non-magnetic samples, placing the NV^- center at the edge of the sample can ensure that the maximum variation of the magnetic flux intensity is obtained as the sample transforms into a superconductor and meanwhile, the arrangement of the exciting coil on the gasket and as close to the sample as possible can maximize the magnetic field within the sample, which endows the NV^- center with an optimal sensitivity for detecting the Meissner effect in the DAC. This work is expected to be useful for detecting the superconductivity of materials under extremely high pressures such as metallic hydrogen.

References

[1] Ashcroft N W 2004 *Phys. Rev. Lett.* **92** 187002
[2] Li Y, Hao J, Liu H, Li Y and Ma Y 2014 *J. Chem. Phys.* **140** 174712
[3] Troyan I, Gavriliuk A, Rüffer R, Chumakov A, Mironovich A, Lyubutin I, Perekalin D, Drozdov A P and Eremets M I 2016 *Science* **351** 1303
[4] Drozdov A P, Eremets M I, Troyan I A, Ksenofontov V and Shylin S I 2015 *Nature* **525** 73
[5] Yao Y and Tse J S 2018 *Chemistry* **24** 1769
[6] Pickett W E 2007 *J. Supercond. Novel Magn.* **19** 291
[7] Takano Y, Takeya H, Fujii H, Kumakura H, Hatano T, Togano K, Kito H and Ihara H 2001 *Appl. Phys. Lett.* **78** 2914
[8] Waxman A, Schlussel Y, Groswasser D, Acosta V M, Bouchard L S, Budker D and Folman R 2014 *Phys. Rev. B* **89** 054509
[9] Yang J, Peng G, Han Y H and Gao C X 2011 *AIP Adv.* **1** 032116
[10] Huang X W, Gao C X, Han Y H, Li M, He C, Hao A, Zhang D, Yu C, Zou G and Ma Y 2007 *Appl. Phys. Lett.* **90** 242102
[11] Huang X W, Gao C X, Li M, He C, Hao A, Zhang D, Yu C, Wang Y, Sang C, Cui X and Zou G T 2007 *J. Appl. Phys.* **101** 064904
[12] Bouchard L S, Acosta V M, Bauch E and Budker D 2011 *New J. Phys.* **13** 025017
[13] Jiang F J, Ye J F, Jiao Z, Jiang J, Ma K, Yan X H and Lv H J 2018 *Chin. Phys. B* **27** 057602
[14] Doherty M W, Struzhkin V V, Simpson D A, McGuinness L P, Meng Y, Stacey A, Karle T J, Hemley R J, Manson N B, Hollenberg L C and Prawer S 2014 *Phys. Rev. Lett.* **112** 047601
[15] Hall L T, Kehayias P, Simpson D A, Jarmola A, Stacey A, Budker D and Hollenberg L C 2016 *Nat. Commun.* **7** 10211
[16] Steinert S, Dolde F, Neumann P, Aird A, Naydenov B, Balasubramanian G, Jelezko F and Wrachtrup J 2010 *Rev. Sci. Instrum.* **81** 043705
[17] Balasubramanian G, Chan I Y, Kolesov R, Al-Hmoud M, Tisler J, Shin C, Kim C, Wojcik A, Hemmer P R, Krueger A, Hanke T, Leitenstorfer A, Bratschitsch R, Jelezko F and Wrachtrup J 2008 *Nature* **455** 648
[18] Hong S, Grinolds M S, Pham L M, Le Sage D, Luan L, Walsworth R L and Yacoby A 2013 *MRS Bull.* **38** 155
[19] Maertz B J, Wijnheijmer A P, Fuchs G D, Nowakowski M E and Awschalom D D 2010 *Appl. Phys. Lett.* **96** 092504
[20] Maze J R, Stanwix P L, Hodges J S, Hong S, Taylor J M, Cappellaro P, Jiang L, Dutt M V, Togan E, Zibrov A S, Yacoby A, Walsworth R L and Lukin M D 2008 *Nature* **455** 644
[21] Wickenbrock A, Zheng H, Bougas L, Leefer N, Afach S, Jarmola A, Acosta V M and Budker D 2016 *Appl. Phys. Lett.* **109** 053505
[22] Yue D H, Ji T T, Qin T R, Wang J, Liu C L, Jiao H, Zhao L, Han Y H and Gao C X 2018 *Appl. Phys. Lett.* **112** 081901
[23] Joshi K R, Nusran N M, Cho K, Tanatar M A, Meier W R, Bud'ko S L, Canfield P C and Prozorov R 2019 *Phys. Rev. Applied* **11** 014035